Volume 16, Issue 4, 162531 (1-14)

International Journal of Nano Dimension (IJND)

https://dx.doi.org/10.57647/j.ijnd.2025.1604.31

Optimizing thermal efficiency: A study on parabolic trough solar collector performance with nanofluids and fin designs

Mostafa Jamali, Najmeh Hajialigol*

Mechanical Engineering Department, Hamedan University of Technology, Hamedan, Iran.

***Corresponding author:** n.hajialigol@hut.ac.ir

Original Research

Received:
20 January 2025
Revised:
14 April 2025
Accepted:
5 May 2025
Published online:
10 May 2025
Published in issue:
17 May 2025

Abstract:

This study comprehensively explores the application of thermal nanofluids in enhancing the performance of solar parabolic trough collectors through advanced computational modeling techniques. Specifically, the research employs the Large Eddy Simulation (LES) model to investigate heat transfer dynamics, focusing on the interplay between fluid flow characteristics and thermal energy distribution. The analysis examines the influence of varying porous fin heights on the flow structure and heat transfer behavior under a wide range of Reynolds numbers ($40,000 - 450,000$) and a fixed Prandtl number of 0.7. Key results indicate that increasing the height of the porous fins significantly improves the overall heat transfer efficiency, as evidenced by an enhancement in the Nusselt number. Additionally, the findings reveal a corresponding increase in the tube friction coefficient, which is essential for understanding the trade-offs between thermal performance and flow resistance. These insights underscore the potential of optimized fin geometries and nanofluid applications in advancing the efficiency of solar thermal power systems.

Keywords: Friction coefficient; Heat transfer; Nanofluid; Nusselt number; Reynolds number; Numerical simulation; Solar parabolic collectors

1. Introduction

Solar energy is an abundant and promising resource capable of meeting a substantial share of global energy needs [1–3]. Despite extensive research on solar energy applications in solar thermal technologies, further studies are essential to address the challenges and limitations inherent in these systems [4–7]. Solar concentrators play a crucial role in converting solar energy into high-temperature heat for solar thermal energy technologies [8–10]. Among concentrated solar energy technologies, the Parabolic Trough Solar Collector (PTC) stands out as the most established and straightforward option, capable of achieving temperatures up to 400 °C using thermal oils [11] and 550 °C with molten salts [12]. PTCs leverage advanced materials with unique bonding characteristics and surface properties to enhance the efficiency of solar energy conversion into heat. This integration of molecular interactions, material properties, and energy optimization bridges multiple research domains [13, 14].

Scholars have developed various analytical models to optimize the thermal efficiency of PTCs. Ouagued [15] introduced a one-dimensional (1-D) model that incorporated the role of working oil by dividing the Heat Collection Element (HCE) into sections. Expanding this concept, Padilla [16] derived control equations for the glass, fluid, and absorber components, which led to the development of one-dimensional and two-dimensional (2-D) models [17]. The key distinction lies in the segmentation of the receiver into multiple segments along the PTC's length in the 2-D approach compared to the 1-D approach. Discussions on these models address assumptions, constraints, enhancement strategies, and physical parameters.

Kalogirou [18] examined heat transfer through the glass cover and absorber pipe, while Odeh [19] evaluated the collector's efficiency based on the temperature of the absorber wall and the working fluids. Kassem [20] suggested that heat transfer could be optimized by adjusting eccentricity

based on studies of natural convection heat transfer between the absorber and glass envelope. Gong [21] refined the 1-D model by integrating it with a three-dimensional (3-D) end model, achieving strong empirical correlation. Lu [22] proposed a non-uniform model that divided the absorber and glass into regions with varying temperatures, employing the Monte Carlo Ray Trace and Finite Volume Method (FVM) [23] to analyze heat transfer dynamics. Cheng [24] identified non-uniform temperature distribution as a critical factor leading to system failure.

In solar energy applications, particularly in PTC systems, advanced materials enhance energy capture and conversion efficiency. Metal-based nanomaterials like nano-ZnO and gold nanocomposites offer potential improvements in catalytic processes for solar energy harvesting and thermal storage. Efficient catalyst development also reduces energy input for chemical processes, aligning them with sustainable solar-driven operations. Furthermore, integrating chemical mechanisms for organic synthesis into solar-driven reactors can enable environmentally-friendly production processes [25–27].

The principal aim of these models is to maximize PTC performance. However, computational duration poses a significant challenge in testing procedures. Numerical methods, such as Computational Fluid Dynamics (CFD), often require extended periods to complete, driving researchers toward simpler, faster, and more precise analytical models. Cheng et al. [28] developed a model to examine non-uniform temperature distribution within the receiver and inconsistent solar flux incidence by dividing the setup into distinct dormant and linear regions. Huang et al. [29] proposed a model evaluating optical efficiency based on light distribution from reflective points. Behar et al. [30] explored tracking modes' effects on thermal efficiency, recommending north-south and east-west orientations as optimal. Ratzel et al. [31] created models addressing heat dissipation through the receiver's annular space, pinpointing conduction and convection as primary contributors and suggesting solutions like using low-conductivity glass and widening the annular gap.

PTCs concentrate direct solar radiation along their focal axis to significantly increase the temperature of heat transfer fluids. A PTC system comprises a parabolic reflector that directs solar radiation onto a linear receiver at its focal point, with solar tracking ensuring precise alignment. The working fluid absorbs concentrated heat while circulating through the receiver. Factors such as fluid velocity, internal heat gain, geometric concentration ratio, and surface heat loss impact the system's efficiency [32]. The receiver design plays a vital role in overall performance. Studies on enhancing PTC efficiency span 1-D, 2-D, and 3-D analyses, employing CFD techniques like finite volume method, boundary element method (BEM), finite element method (FEM), and finite difference method (FDM) [33].

Shuai et al. [34] utilized FEM and Monte Carlo ray tracing (MCRT) to model PTCs performance, revealing that radial stresses were minimum compared to axial stress. They observed that stainless steel and SiC exhibit higher radial stresses and temperature gradients than Cu and Al. Their findings also suggested that thermal stress could be reduced by 46.6% by using eccentric tube receivers. Tripathy et al. [35] investigated the material impact on a PTC absorber tube using FVM, concluding that the heat transfer rate was unaffected by the absorber tube material. They discovered that Cu-Al-SiC-Fe and Cu-Fe composites could reduce maximum deflection by $45-49\%$ and $7-15\%$, respectively, in comparison to steel. Kassem [36] applied FDM to estimate the convective heat transfer rate in the annulus between the glass cover and receiver of a parabolic-cylindrical solar collector, deducing that optimal eccentricity selection could enhance heat transfer and decrease the local Nusselt number with increased eccentricity.

Kumar et al. [37] examined the receiver tube alongside porous discs within a linear solar parabolic trough collector, assessing the influence of receiver design, solar radiation concentration, and thermic fluid properties on heat collection. They reported that a receiver featuring a top porous disc configuration (where $(w = di)$, $(H = 0.5di)$, and $(h = 30)$) exhibited superior heat transfer capabilities, improving by approximately 64.3% with a pressure drop of 457 Pa compared to a standard tubular receiver. They also noted a significant enhancement in system performance due to the incorporation of porous media in tubular solar receivers.

Gunes et al. [38] conducted experimental research on pressure drop and heat transfer in a turbulent flow regime through a tube fitted with coiled wire inserts. Their studies indicated that coiled wire inserts markedly increase pressure drop and heat transfer compared to smooth tubes. Additionally, they found that the Nusselt number improved with thicker wires, higher Reynolds numbers, and lower pitch ratios. The most efficient overall enhancement, at 36.5%, was achieved with a wire characterized by $(P/D = 1)$ and $(a/D = 0.0892)$ at a Reynolds number of 3858.

Bellos et al. [39] posited that employing nanofluids, internal fins, and a combination of both could boost thermal efficiency by 0.76%, 1.10%, and 1.54%, respectively. In subsequent research, Bellos et al. [40] explored the effects of reflective shields and internal longitudinal fins. They found that internal fins consistently yield thermal gains, while radiant shields prove beneficial at elevated temperatures.

Traditional PTCs focus solar radiation at the absorber base of tube, leading to deformation, thermal stress, and high temperatures. Norouzi et al. [41] suggested rotating the absorber tube at a specific frequency to mitigate high surface temperatures and enhance solar energy absorption. They also experimental a nanofluid (Al_2O_3-Therminol) as the heat transfer fluid. Their proposed 2D-transient model of PTCs, along with 3-D steady laminar numerical simulations showed that aluminium is the optimal material for the absorber tube, yielding an output temperature approximately 16 K higher—nearly 5% more than steel. This approach also resulted in a more uniform surface temperature distribution and improved the collector's thermal efficiency.

Increasing the effective heat transfer surface area is a common and effective strategy to enhance heat transfer, though it may increase pressure drop. Guidance fins and porous

media are potent methods to augment the effective surface area and thus heat transfer [41]. Rashidi et al. [42] provided a thorough review of porous material applications in solar energy systems. At the same time, other studies have considered gradient porous properties to boost heat transfer with minimal pressure losses [43–45].

Viswanathan et al. [46] investigated turbulent flow in a fixed finned tube with a 180° bend using numerical methods, comparing the Detached Eddy Simulation (DES) model results with those of the Large Eddy Simulation (LES) model and experimental data. The DES model demonstrated a reasonable error margin relative to the LES model's numerical and experimental outcomes, also significantly reducing computation time. The study by Ray et al. [47] explored the influence of inlet temperature of the heat transfer fluid (HTF) and wind velocity on the performance of a parabolic trough solar collector receiver. They observed that as the inlet temperature increased from 363 °K to 663 °K, the circumferential temperature difference (ΔT_c) decreased from 30.49 °K to 17.08 °K, while the thermal efficiency of the receiver declined by 6.45%. Moreover, an increase in wind velocity over the receiver's glass cover, from 0.5 m/s to 5 m/s, led to an 8.59% reduction in the glass cover's peak temperature.

Asish Sarangi et al. [48] reviewed various working fluids utilized in the receiver tube of parabolic trough solar collectors, focusing on the stability, manufacturing techniques, and impacts of hybrid nanofluids on the thermal properties of PTSCs. Hybrid nanofluids and conventional nanofluids were identified as potential options for enhancing the thermal and optical properties of PTSCs. Their findings indicated that metal oxide hybrid nanofluids demonstrated superior efficiency in improving thermal conductivity and heat transfer compared to oxide nanofluids. This research provides valuable guidance for scientists and manufacturers in selecting suitable working fluids for PTSC applications.

Yanjuan Wang et al. [49] analyzed the performance of a parabolic trough solar collector (PTC) under non-uniform solar flux conditions using numerical methods such as solar ray tracing (SRT) and finite element modeling (FEM). Their findings revealed that the circumferential temperature difference (CTD) of the absorber decreased with increasing inlet temperatures and fluid velocities but rose with higher direct normal irradiance (DNI). For inlet velocities of $1.00-4.00$ m/s, DNIs ranging from $500-1250$ W/m^2, and inlet temperatures between 373 °K and 673 °K, the CTD ranged from 22 °K to 94 °K. Additionally, thermal stress and deformation were found to be more pronounced in the absorber than in the glass cover. These insights contribute to optimizing PTC designs for solar thermal power plants in China.

Yu Qiu et al. [50] investigated the thermal performance and heat transfer characteristics of a parabolic trough solar collector using supercritical CO_2 (s-CO_2) as the HTF under non-uniform solar flux. Their study applied a detailed three-dimensional Monte Carlo ray tracing (MCRT) and finite volume method (FVM) model to analyze energy transfer in the collector. Two typical conditions for the s-CO_2 Brayton and Rankine cycles were examined, offering critical insights into the application of s-CO_2 in enhancing PTC performance.

This research employs computational modeling to examine the use of thermal nanofluids in a solar parabolic trough collector. Turbulent fins, which are a type of extended surface, enhance the heat transfer coefficient and Nusselt number for fluid flow within the tube. Additionally, they help to lower the pressure drop and drag force on the tube compared to plain or perforated fins. Despite advancements in solar thermal systems, limited studies address the combined influence of nanofluids and innovative fin geometries on thermal and flow performance in parabolic trough collectors. This study bridges this research gap by numerically analyzing the geometry of turbulent fins and their effects on flow and heat transfer characteristics. The novelty of the work lies in its focus on integrating thermal nanofluids with optimized fin designs to achieve superior heat transfer efficiency and reduced flow resistance. The findings provide valuable insights for the design and optimization of parabolic trough solar collector receiver tubes equipped with these advanced fin configurations.

2. Materials and methods

Fig. 1 illustrates the detailed geometry of the solar collector, emphasizing the strategic arrangement of trapezoidal fins designed to enhance heat transfer performance. The collector's configuration includes a total of 84 trapezoidal fins, evenly distributed in three rows, each consisting of 28 fins. The precise spacing of 66 mm between adjacent fins has been carefully selected to strike an optimal balance between maximizing thermal performance and minimizing pressure drop within the system. This systematic arrangement ensures efficient absorption and transfer of solar energy, thereby improving the overall thermal efficiency of the collector.

The schematic also highlights the integration of the fins with the absorber tube, showcasing how their geometry plays a pivotal role in enhancing the flow dynamics of the heat transfer fluid (HTF). By increasing the surface area for heat exchange and promoting turbulence in the fluid flow, these fins contribute significantly to the augmentation of the heat transfer coefficient and the reduction of thermal resistance. This layout not only facilitates effective heat dissipation but also addresses challenges associated with pressure losses, ensuring reliable and efficient operation of the solar collector.

The large eddy simulation is used in this study. The governing continuity, momentum, and energy equation is written as [51].

$$\frac{\partial}{\partial x_j}(\bar{\rho}\tilde{u}_j) = 0 \tag{1}$$

$$\frac{\partial}{\partial x_j}(\bar{\rho}\tilde{u}_i\tilde{u}_j) = -\frac{\partial \bar{P}}{\partial x_i} + \frac{\partial}{\partial x_j}(2(\mu_{nf}+\bar{\mu}_{SGS})[\tilde{S}_{ij} - \frac{1}{3}\delta_{ij}\tilde{S}_{kk}]) \tag{2}$$

$$\frac{\partial}{\partial x_j}(\bar{\rho}\tilde{u}_j\tilde{h}) = \frac{D\bar{P}}{Dt} + \frac{\partial}{\partial x_j}((\frac{\mu_{nf}}{Pr} + \frac{\bar{\mu}_{SGS}}{Pr_t})\frac{\partial \tilde{h}}{\partial x_j}) \tag{3}$$

The modeling was carried out symmetrically due to the symmetrical shape of the solar collector, which is a cylinder with a length of 2 m. The walls into which the heat flux

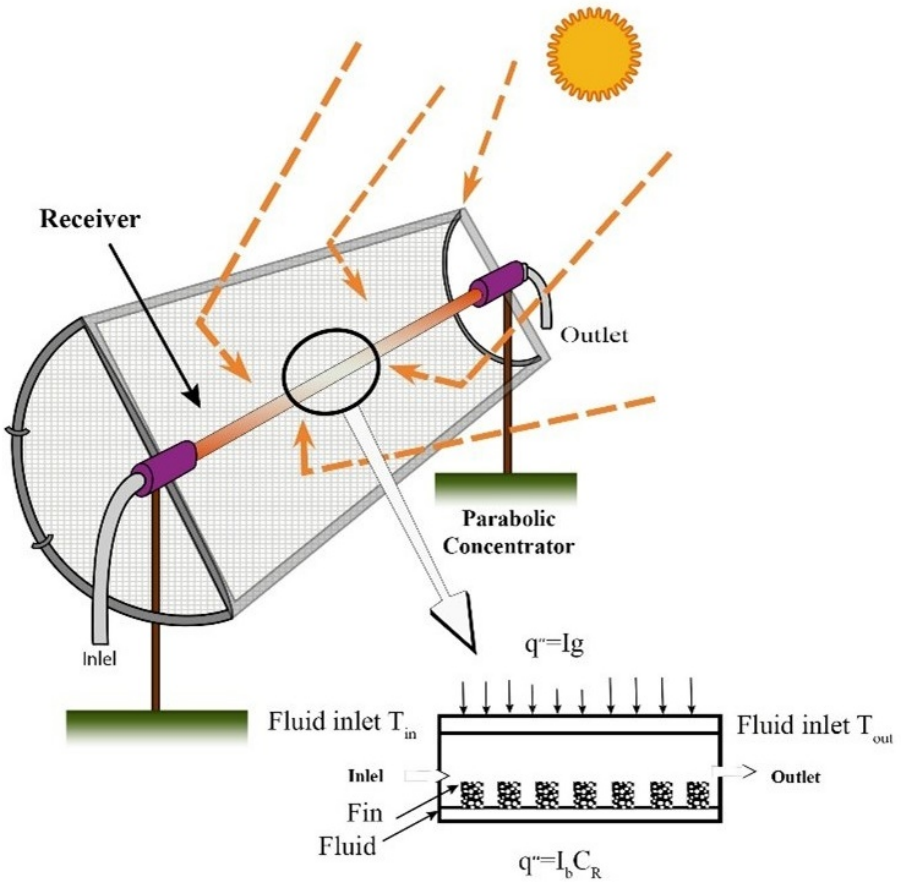

Figure 1. Geometry of solar collector with fins.

enters were divided into two parts. The upper surface is directly heated by radiation, but the heat flux of the lower surface is due to radiation caused by reflection.

The physical characteristics of the working fluid (water) were considered. The inlet velocity perpendicular to the surface is one of the boundary conditions of the inlet flow. The walls have a no-slip condition. A constant heat flux was considered to simulate the heating elements on the walls. The effect of wall roughness has been ignored due to the insignificance of wall roughness compared to the presence of fin.

In the lower half of the receiver, the distribution of uniform heat flux is:

$$q'' = I_b C_R,\ r = \frac{D}{2},\ -90 \le \theta \le 0, 0 \le L \le 2 \qquad (4)$$

In the upper half of the receiver, the uniform heat flux distribution is:

$$q'' = I_g,\ r = \frac{D}{2},\ 0 \le \theta \le 90, 0 \le L \le 2 \qquad (5)$$

$$I_g = 750\text{W/m}^2,\ I_b = 600\text{W/m}^2$$

$$C_R = \frac{A_p}{A_r}$$

where C_R is the concentration ratio of the concentrator, I_b is the concentrated beam intensity, I_g is the intensity of the sun's radiation, A_r is the collector receiver area, and A_P is the collector concentrator area.

The friction coefficient of the tubes with solid and porous fins was calculated from Eq. (7).

$$f = \frac{\Delta p_e}{\rho U_m^2/2}\frac{D}{L} \qquad (6)$$

where Δp_e is the effective pressure drop and it is obtained from Eq. (7) in straight-finned tubes:

$$\Delta p_e = p_{in} - p_{out} + \frac{1}{2}\rho U_{in}^2 - \frac{1}{2}\rho U_{out}^2 \qquad (7)$$

$$U_{in} = U_{out}$$

Eqs. (8) and (9) express the changes in the pressure drop and overall heat transfer coefficient in various mass fluxes for the tube with a porous trapezoidal fin.

$$h_{nf} = \frac{q''}{T_{wall} - T_{nf}} \qquad (8)$$

$$Nu = \frac{h_{nf} D_e}{k_{nf}} \qquad (9)$$

Finally, the thermal performance factor (TPF) represents the parameter that summarizes the thermal improvement and increases in pressure drop compared to the reference case (smooth model) and provides details about the net energy gain of the system. This factor can be written as follows

$$\text{TPF} = \left(\frac{Nu}{Nu_0}\right)\left(\frac{f_0}{f}\right)^{\frac{1}{3}} \qquad (10)$$

Table 1. Geometric parameters of the receiver and fin.

Receiver inside diameter (mm)	$D = 66$
Receiver length (mm)	$L = 2000$
Square fin thickness (mm)	$W = 4$
Distance between two fins (mm)	$P = 66$
Trapezoidal shape fin (top and bottom thickness ratio)	$\lambda = 0.25$

Table 2. Characteristics of working fluid, solid fins and nanoparticles.

Property	Working fluid	Solid fin	Nanoparticle (Al_2O_3)
Density (kg/m^3)	938	8027	3970
Specific heat (J/kg K)	1970	500	765
Thermal conductivity (W/m K)	0.118	20	40
Viscosity (N s/m^2)	0.000486	-	-

Table 3. Properties of the porous fins.

Property	Porous fin
Porosity	$\phi = 0.37$
Permeability	$K_p = 2.9 \times 10^{-10}$

The geometric parameters of the receiver, the characteristics of the solid fin and the working fluid, as well as the properties of the porous fin, are given in Tables 1-3, respectively.

Grid independence

Using an index known as LES_{IQk} presented by Pope [52] and validation in other studies [53, 54], the solution grid independency was examined, demonstrated as:

$$\text{LES}_{IQk} = \frac{k^{res}}{k^{tot}} \tag{11}$$

Regarding the equations, k^{res} denotes the resolved kinetic energy, while k^{tot} represents the overall kinetic energy. Previous studies have suggested that for high Reynolds numbers flows, an appropriate range could be between 75% and 85% [42]. To determine a cost-effective and optimal mesh configuration, different grid sizes were evaluated. For having an affordable and precise grid, various cell numbers have been examined and finally, the cell number of about 1528000 is chosen. In geometry with this number of cells LES_{IQk} is 0.91.

Validation

To verify the validity of the derived scientific model and the precision of the numerical outputs in the present study, it is necessary to correlate the previously reported results. In this research, the results of Reddy et al. [27] were used. The changes of Nusselt number in different mass flow rate for solid and porous trapezoidal tubes and comparison with numerical work of Reddy et al. can be seen in Figs. 2 and 3. The supreme variation between the results is less than 8%. Therefore, the current numerical procedure can capture the valid results.

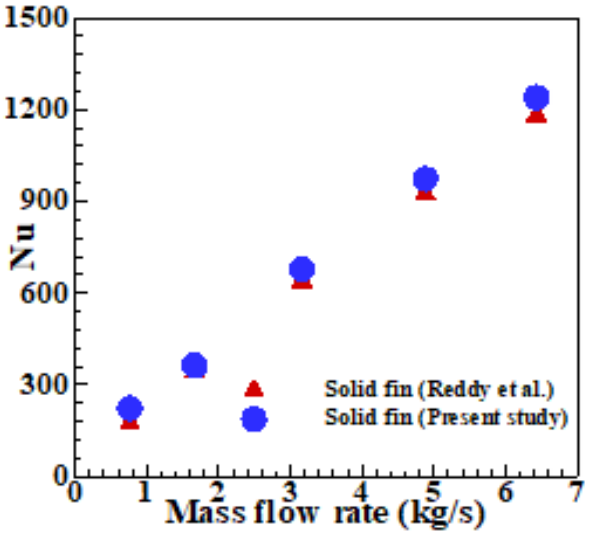

Figure 2. Comparison of overall Nusselt number in different mass flow rate of solid trapezoidal tube with numerical results of Reddy et al.[13].

3. Results and discussion

3.1 Effect of fin height on the tube cross-section

3.1.1 Pressure contour

Figure 4 presents the pressure contours obtained from a 3D simulation at a Reynolds number of 400,000 for trapezoidal finned tubes with varying fin heights of 4 mm, 8 mm, and 12 mm. The data reveal that as fin height increases, the wall's resistance to flow along the tube also increases. This elevated resistance causes intensified flow turbulence and greater energy dissipation, which ultimately results in a

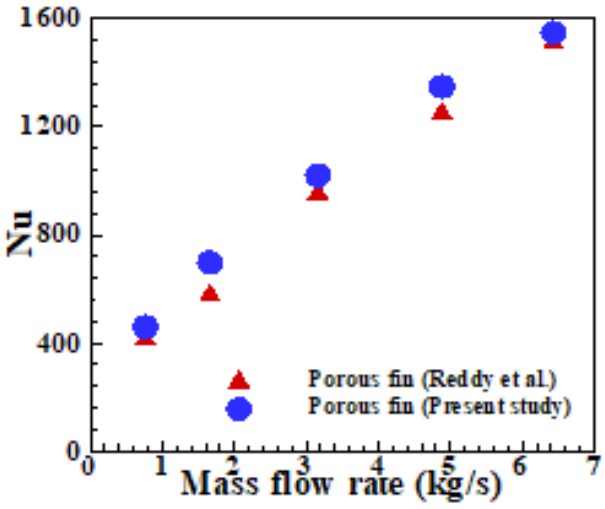

Figure 3. Comparison of overall Nusselt number in different mass flow rate of porous trapezoidal tube with numerical results of Reddy et al.[27].

higher pressure drop across the tube.

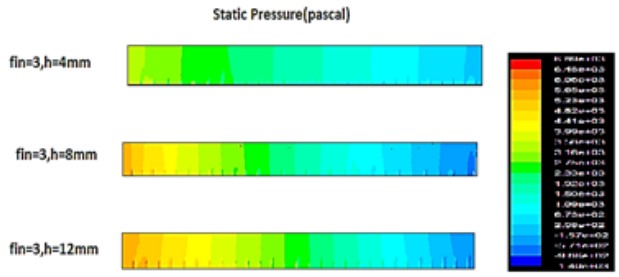

Figure 4. Comparison of pressure contours in 3D simulation at Reynolds 400,000 for trapezoidal finned tubes with heights of 4, 8, and 12 mm.

Extended analysis:

1. Flow Resistance: Taller fins significantly increase the surface area interacting with the fluid flow. This leads to higher flow resistance, as the fins impede the movement of fluid more effectively compared to shorter fins. The added resistance impacts the velocity profiles and flow stability within the tube.

2. Turbulence and Energy Dissipation: The enhanced fin height promotes turbulence, which plays a key role in improving heat transfer efficiency. However, it also increases energy dissipation, as turbulent flows consume more energy to sustain their movement. This relationship demonstrates the dual effect of fins-beneficial for heat transfer but challenging in terms of energy efficiency.

3. Pressure Drop: The combined impact of increased flow resistance and heightened turbulence culminates in a significantly greater pressure drop across the tube. This rise in pressure drop is a critical factor in the overall system design, as it affects the operational energy requirements and flow behavior.

These findings hold substantial importance for optimizing the receiver tube design in parabolic trough solar collectors. They underscore the trade-offs between enhanced thermal performance due to improved heat transfer and the increased pressure drop that accompanies fin modifications. A comprehensive understanding of these dynamics is essential for developing receiver systems that achieve an optimal balance between energy efficiency, thermal performance, and operational feasibility. Researchers and engineers can leverage this knowledge to refine designs and choose fin dimensions that align with specific application needs, ensuring sustainable and cost-effective solutions for solar thermal energy systems.

3.1.2 Velocity contour

Figure 5 illustrates the contours of the absolute value of velocity obtained from a 3D simulation at a Reynolds number of 400,000 for trapezoidal finned tubes with fin heights of 4 mm, 8 mm, and 12 mm. The simulation reveals that as the fin height increases, the boundary layer grows thicker, significantly influencing fluid flow dynamics within the tube and leading to a noticeable reduction in the velocity of the fluid.

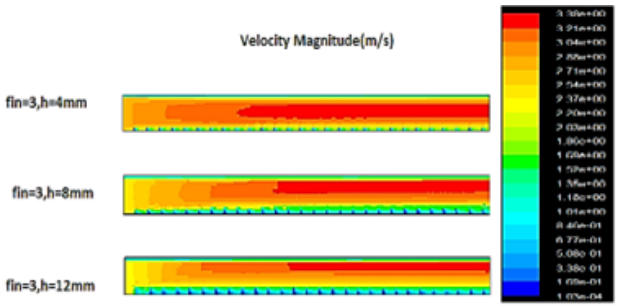

Figure 5. Comparison of contours of the absolute value of the velocity at Reynolds 400,000 for trapezoidal finned tubes with heights of 4, 8 and 12 mm.

Extended observations:

1. Boundary Layer Development: The increase in fin height results in a more substantial expansion of the boundary layer. This phenomenon alters the flow characteristics by creating regions of slower-moving fluid near the surface of the fins, impacting the stability and uniformity of flow throughout the tube.

2. Velocity Reduction: As the boundary layer thickens, the velocity of the fluid decreases due to increased interaction between the fluid and the larger surface area of the fins. This heightened frictional resistance slows down the fluid, affecting its overall momentum and flow efficiency.

3. Impact on Flow Dynamics and Heat Transfer: While the reduction in fluid velocity may challenge flow efficiency, the presence of taller fins contributes to enhanced turbulence within the boundary layer. This turbulence can improve heat transfer rates by encouraging more vigorous interaction between the fluid and the finned surfaces.

4. Trade-Offs and System Optimization: These findings underscore the importance of fin geometry in balancing the performance metrics of parabolic trough solar collector systems. Taller fins promote better heat transfer but also increase flow resistance, which must be carefully managed to prevent excessive energy loss and ensure optimal system operation.

Understanding these fluid dynamics and their implications for heat transfer is vital for designing efficient receiver tubes in parabolic trough solar collectors. By tailoring fin dimensions to align with specific operational requirements, engineers and researchers can achieve a balanced approach that maximizes thermal efficiency while minimizing energy consumption and fluid flow resistance. These insights pave the way for advancements in solar thermal technologies and sustainable energy systems.

3.1.3 Heat transfer and pressure drop

Figure 6 illustrates the impact of increasing fin height in the tube cross-section on the overall heat transfer coefficient across the tube at various Reynolds numbers (460,000, 380,000, 310,000, 230,000, 150,000, 80,000, and 60,000). The results demonstrate a significant interplay between fin geometry, flow behavior, and thermal performance. As the fin height increases, the fluid reaches and interacts with taller fins, resulting in the formation of larger longitudinal vortices within the flow. These vortices enhance the mixing of fluid layers, which is crucial for improving heat transfer performance. The stronger secondary flows generated around taller fins contribute to a noticeable rise in the overall heat transfer coefficient, making the system more efficient in transferring thermal energy. However, this improvement in heat transfer comes with trade-offs. The increased fin height leads to a greater resistance to fluid flow along the tube. This resistance is caused by the larger surface area of the fins, which interacts more extensively with the fluid and creates additional friction. The enhanced interaction not only impedes the flow but also induces higher levels of turbulence and energy dissipation within the system.
Consequently, these factors collectively result in a significant increase in the pressure drop within the tube. The greater energy required to overcome flow resistance must be carefully accounted for when designing such systems, as excessive pressure drops can lead to higher operational costs and reduced overall efficiency. These findings highlight the dual effects of increasing fin height: enhanced heat transfer efficiency due to improved fluid mixing and turbulence, balanced against the drawbacks of higher flow resistance and pressure loss. By analyzing the relationship between fin height, heat transfer, and pressure drop, engineers and researchers can optimize the design of receiver tubes for parabolic trough solar collectors. Such optimization aims to maximize thermal performance while minimizing energy consumption, ensuring a balanced and efficient system for renewable energy applications. This comprehensive understanding provides valuable insights into the trade-offs inherent in fin geometry adjustments, guiding the development of more sustainable and effective thermal systems.

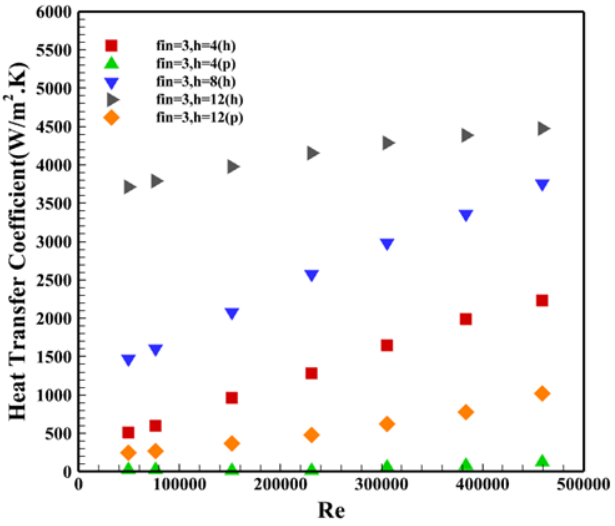

Figure 6. Comparison of heat transfer coefficient in porous trapezoidal finned tubes with heights of 4, 8, and 12 mm at different Reynolds numbers.

3.1.4 Overall Nusselt number

Figure 7 illustrates the variation of the overall Nusselt number at different Reynolds numbers for trapezoidal finned tubes with fin heights of 4 mm, 8 mm, and 12 mm. The results indicate that as the Reynolds number increases, the secondary flows intensify, resulting in stronger longitudinal vortices within the flow. These vortices significantly enhance the mixing of fluid layers, improving the heat transfer process and leading to a corresponding rise in the Nusselt number. This highlights the critical role of secondary flow dynamics in optimizing the thermal performance of finned tube systems. Notably, at the start of the tube, the heat transfer coefficient is exceptionally high due to the pronounced temperature gradient between the fluid and the tube wall. However, as the fluid moves along the tube, the thermal boundary layer gradually develops and thickens. This thickened boundary layer acts as a thermal resistance, reducing the temperature gradient and subsequently causing a decline in the heat transfer coefficient. This phenomenon is reflected in the slope of the Nusselt plot, which becomes less steep as the Reynolds number increases. Additionally, the results reveal the interplay between fin height and thermal performance. Taller fins provide larger surface areas for heat exchange, which enhances heat transfer efficiency. However, they also introduce greater flow resistance, which can impact overall fluid dynamics. The interplay between these factors emphasizes the importance of selecting appropriate fin dimensions to balance heat transfer performance and flow resistance effectively.
As the fin height increases, the interaction between the fluid and the finned surfaces becomes more pronounced, leading to the emergence of stronger secondary flows. These secondary flows, characterized by turbulent and irregular movements of fluid particles, play a crucial role in enhancing the heat transfer process. The turbulence promotes efficient mixing of the fluid layers, reducing thermal resistance and facilitating greater energy transfer from the heated surface to the fluid. Consequently, the overall Nusselt num-

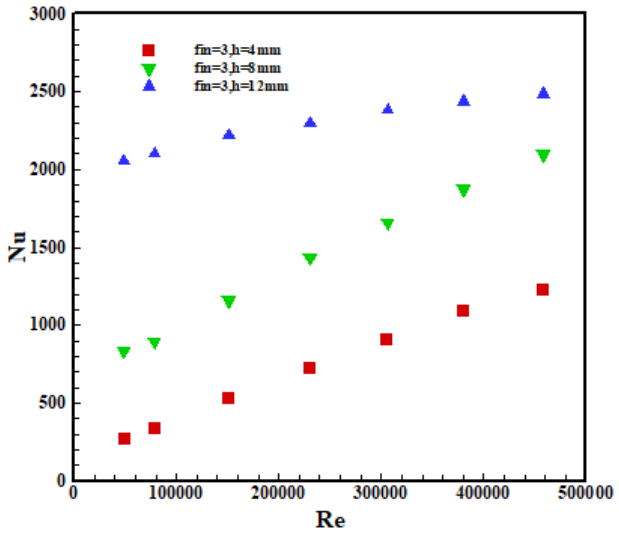

Figure 7. The overall Nusselt number for trapezoidal finned tubes with heights of 4, 8, and 12 mm at different Reynolds numbers.

ber experiences a significant rise, reflecting improved heat transfer performance. Additionally, the increased fin height creates larger surface areas for heat exchange, further amplifying the impact of the secondary flows on the heat transfer mechanism. The combined effects of intensified turbulence, enhanced fluid mixing, and greater surface interaction collectively result in a notable improvement in the thermal efficiency of the system. However, it is also important to recognize the trade-offs associated with these effects. While taller fins lead to better heat transfer and higher Nusselt numbers, they also contribute to increased flow resistance within the tube. This heightened resistance can lead to greater energy dissipation and a higher pressure drop, which must be accounted for when designing efficient systems. By carefully balancing fin height with operational requirements, it is possible to optimize both heat transfer performance and system efficiency. These findings underscore the importance of understanding the interplay between fin geometry, secondary flow dynamics, and thermal properties in engineering applications.

3.1.5 Overall friction coefficient

Figure 8 illustrates the variation in the friction coefficient for three trapezoidal finned tubes with fin heights of 4 mm, 8 mm, and 12 mm at different Reynolds numbers. The analysis reveals a notable relationship between Reynolds number, fin height, and flow dynamics within the tubes. As the Reynolds number increases, the friction coefficient decreases significantly. This reduction can be attributed to the diminishing influence of wall and viscosity effects on the fluid flow. Higher Reynolds numbers correspond to more turbulent flows, where inertial forces dominate over viscous forces, thereby reducing the impact of viscosity and wall friction on the overall flow resistance. This phenomenon highlights the dynamic nature of fluid behavior as velocity increases. On the other hand, increasing the height of the fins introduces a more complex interaction between the flow and tube walls. Taller fins enhance surface area and intensify flow turbulence, leading to greater dissipation and resistance. Consequently, the friction coefficient increases as fin height increases, reflecting the enhanced influence of wall and viscosity effects. This underscores the trade-offs between enhanced heat transfer and increased flow resistance when modifying fin geometry. Additionally, when Reynolds number is elevated across all three tubes, the viscosity effects diminish further, resulting in a consistent decrease in the friction coefficient. The gradual decline in viscous dominance at higher flow rates enhances flow efficiency but requires careful consideration of energy loss due to turbulence and resistance in the system. These findings emphasize the importance of understanding the interplay between Reynolds number, fin height, and fluid dynamics in optimizing the design of thermal systems. By tailoring fin geometry to specific operating conditions, engineers and researchers can achieve a balanced approach that maximizes heat transfer efficiency while minimizing pressure loss and flow resistance.

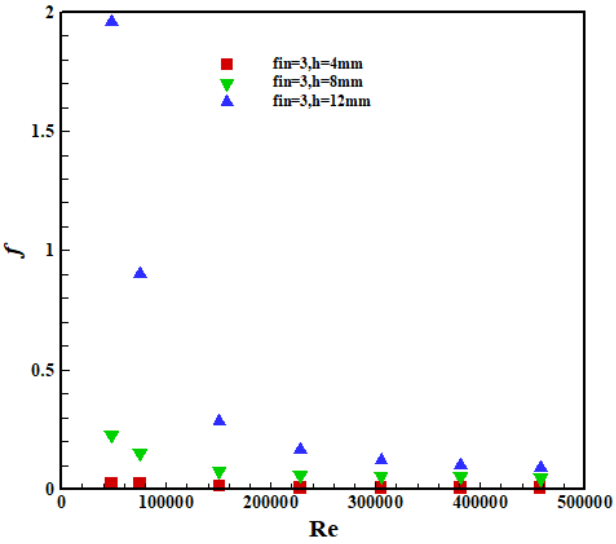

Figure 8. The friction coefficient for three trapezoidal finned tubes with heights of 4, 8, and 12 mm at different Reynolds numbers.

3.2 Effect of the fin number on the tube cross-section

3.2.1 Pressure contour

Figure 9 depicts the pressure contours obtained from a 3D simulation at a Reynolds number of 400,000 for trapezoidal finned tubes with varying numbers of fins 3, 6, and 9 fins. The simulation provides valuable insights into the effect of fin quantity on flow dynamics and pressure characteristics within the tube. As the number of fins increases, the interaction between the fluid flow and the tube walls becomes more complex and intense. This increase in fin count significantly enhances the resistance of the walls against the flow along the tube. The added surface area from additional fins creates more opportunities for the fluid to encounter obstacles, increasing friction and slowing the flow. This heightened resistance is closely tied to the emergence and intensification of secondary flows and turbulence within the tube. The increased turbulence results in a greater level of fluid mixing and dissipation of energy. While turbulence

can be beneficial for improving heat transfer efficiency, it also contributes to higher energy loss within the system. As a direct consequence of these combined effects enhanced resistance, stronger turbulence, and greater dissipation the pressure drop across the tube rises markedly with the addition of more fins.

Furthermore, the results emphasize the trade-offs associated with increasing the number of fins in thermal systems. While additional fins can enhance thermal performance by promoting better heat exchange, they also lead to higher flow resistance and pressure losses, which must be carefully managed. Engineers and researchers can use this information to optimize fin designs, balancing heat transfer efficiency with energy consumption to achieve the desired performance for applications such as parabolic trough solar collectors. These findings underline the importance of understanding the relationship between fin geometry, fluid dynamics, and pressure characteristics. By tailoring fin designs to specific operational conditions, systems can be designed to maximize efficiency while minimizing potential drawbacks, contributing to more sustainable and effective solutions in thermal applications.

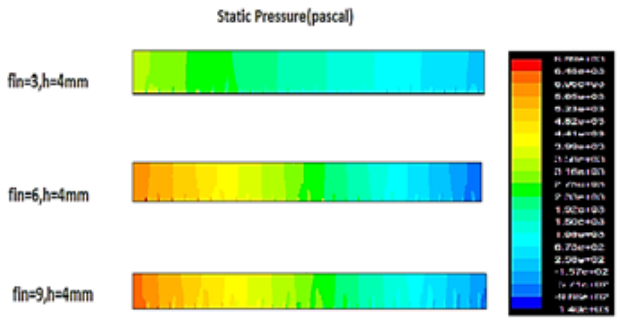

Figure 9. Comparison of pressure contours in 3D simulation at Reynolds 400,000 for trapezoidal finned tubes with fin number of 3, 6, and 9.

3.2.2 Velocity contour

Figure 10 illustrates the contours of the absolute value of velocity obtained from a 3D simulation at a Reynolds number of 400,000 for trapezoidal finned tubes with varying numbers of fins 3, 6, and 9 fins. The results reveal important insights into the influence of fin number on boundary layer development and fluid velocity within the tube. As the fin number increases, the interaction between the fluid and the tube walls becomes more pronounced, leading to a substantial growth in the boundary layer. With more fins, the surface area exposed to the fluid increases significantly, creating additional frictional resistance and impacting the flow dynamics. The thicker boundary layer near the walls not only alters the velocity profile but also introduces more regions of slower-moving fluid within the tube. This increase in the boundary layer thickness directly results in a reduction in fluid velocity. The additional fins impose greater resistance on the flow, causing the fluid particles to move slower. While this reduction in velocity may appear disadvantageous from a flow efficiency perspective, it also contributes to enhanced mixing and turbulence within the boundary layer, which can improve heat transfer in thermal systems.

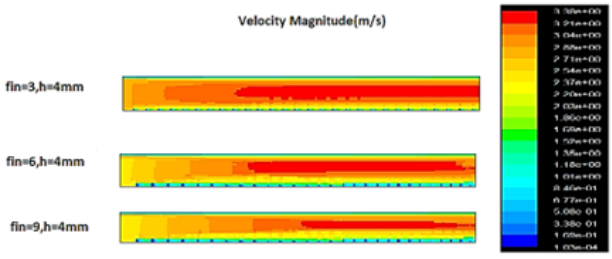

Figure 10. Comparison of contours of the absolute value of the velocity at Reynolds 400,000 for trapezoidal finned tubes with fin number of 3, 6, and 9.

3.2.3 Heat transfer and pressure drop

Figure 11 provides a detailed representation of the impact of increasing the number of fins in the tube cross-section on the overall heat transfer coefficient at varying Reynolds numbers. The results underscore the significant interplay between fin geometry, flow dynamics, and thermal performance within the system. As the number of fins increases, the collision surface between the fluid and the finned surfaces grows, promoting enhanced interactions. This escalation in surface interaction amplifies flow turbulence and facilitates better mixing of the fluid layers, both of which are key contributors to improving heat transfer efficiency. Accordingly, the overall heat transfer coefficient rises, reflecting the system's improved ability to transfer thermal energy effectively. The increased fin number also promotes the formation of larger longitudinal vortices within the flow. These vortices enhance the mixing of fluid in the cross-sectional area of the tube, further improving heat transfer. The stronger secondary flows and turbulence induced by additional fins play a crucial role in augmenting the thermal performance of the system. However, there are trade-offs associated with the increase in fin number. The addition of more fins reduces the cross-sectional area available for fluid flow, leading to an elevated resistance along the walls of the tube. This increased wall resistance, combined with intensified turbulence and dissipation, results in a significant rise in the pressure drop across the tube. A higher pressure drop indicates a greater energy requirement to maintain the flow, which must be carefully managed to prevent excessive operational costs.

3.2.4 Overall Nusselt number

Figure 12 presents the relationship between the overall Nusselt number and Reynolds numbers for trapezoidal finned tubes with fin counts of 3, 6, and 9. The findings reveal key trends in thermal performance and flow behavior as influenced by Reynolds number and fin geometry. As the Reynolds number increases, the Nusselt number also rises, indicating improved heat transfer at higher flow velocities. However, the slope of this increase diminishes with further growth in Reynolds number. This behavior suggests that while the effects of enhanced turbulence continue to improve heat transfer, the rate of improvement slows as inertial forces begin to dominate over viscous forces, reducing the overall efficiency gains.

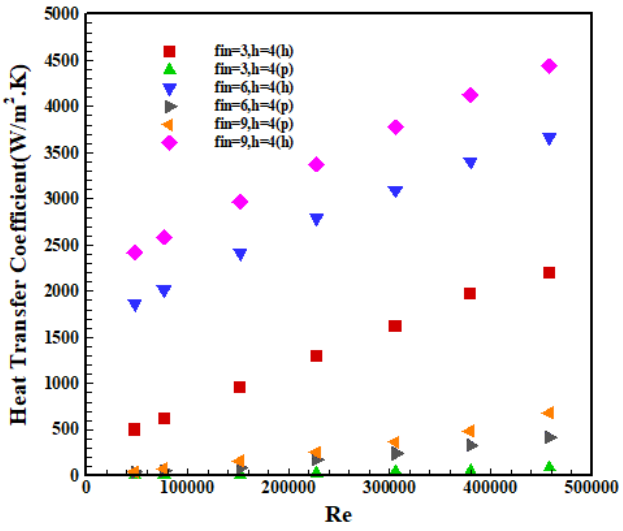

Figure 11. Comparison of heat transfer coefficient in porous trapezoidal finned tubes with fin number of 3, 6, and 9 at different Reynolds numbers.

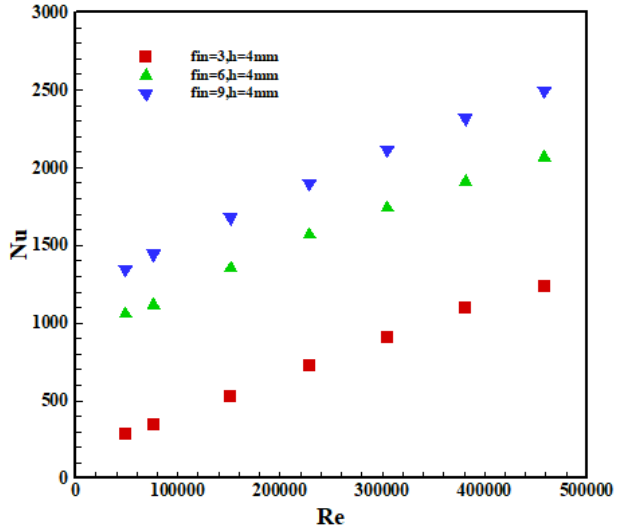

Figure 12. Comparison of the overall Nusselt number for trapezoidal finned tubes with fin number of 3, 6 and 9 at different Reynolds numbers.

Furthermore, the results show that the Nusselt number increases with a higher number of fins. The addition of fins amplifies the available collision surface for fluid interactions, which in turn intensifies the turbulence within the flow. This heightened turbulence enhances the mixing of fluid layers, effectively reducing thermal resistance and boosting heat transfer. As a result, tubes with more fins achieve significantly higher Nusselt numbers, demonstrating superior thermal performance. The increase in the number of fins also facilitates the formation of stronger secondary flows, including larger longitudinal vortices. These vortices play a crucial role in enhancing the fluid mixing process, further contributing to the improved heat transfer coefficient and overall Nusselt number. The synergy of increased surface area, intensified turbulence, and enhanced fluid dynamics underscores the benefits of using more fins for thermal optimization. However, it is important to consider the accompanying trade-offs. While a greater number of fins boost heat transfer efficiency, it also introduces higher flow resistance and potentially increases pressure drop across the tube. This emphasizes the need for careful balancing between thermal performance and flow resistance when designing such systems.

3.2.5 Overall friction coefficient

Figure 13 illustrates the variation of the friction coefficient for trapezoidal finned tubes with fin heights of 4 mm, 8 mm, and 12 mm across a range of Reynolds numbers. The results provide valuable insights into the relationship between flow dynamics, fin geometry, and frictional behavior within the tube system. As the Reynolds number increases, the friction coefficient exhibits a consistent downward trend. This reduction is primarily attributed to the diminishing influence of wall and viscosity effects on the fluid flow at higher Reynolds numbers. In such conditions, inertial forces dominate over viscous forces, reducing the relative contribution of wall friction to the overall resistance. The decrease in the viscosity effects as the flow transitions toward a more turbulent regime plays a significant role in lowering the friction coefficient.

Conversely, as the fin height increases, the friction coefficient experiences a noticeable rise. Taller fins introduce a larger surface area for the fluid to interact with, enhancing the effects of wall resistance and fluid viscosity. The increased surface area also intensifies energy dissipation within the flow, particularly due to stronger turbulence and secondary flow structures induced by the finned geometry. These factors collectively contribute to the higher friction coefficient observed with taller fins. Even as Reynolds number increases for all three fin configurations, the effects of viscosity and wall interactions continue to diminish. This is evident in the consistent reduction of the friction coefficient with higher Reynolds numbers, regardless of fin height. However, the absolute friction coefficient remains higher for tubes with taller fins due to their inherently greater wall resistance and dissipation effects.

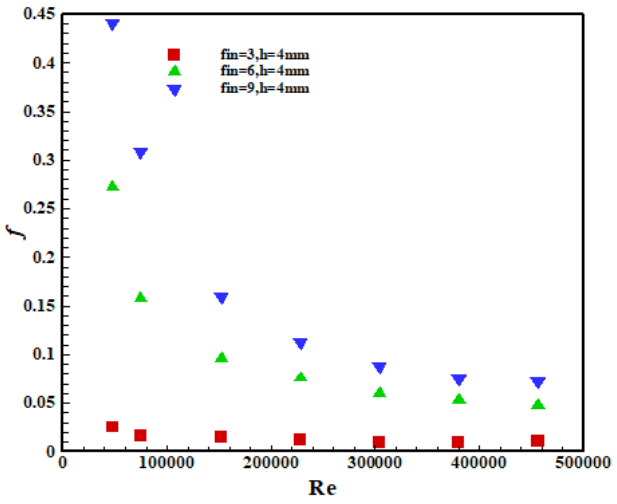

Figure 13. The friction coefficient for three trapezoidal finned tubes with fin number of 3, 6 and 9 at different Reynolds numbers.

Figure 14 illustrates the variation of the relative Nusselt

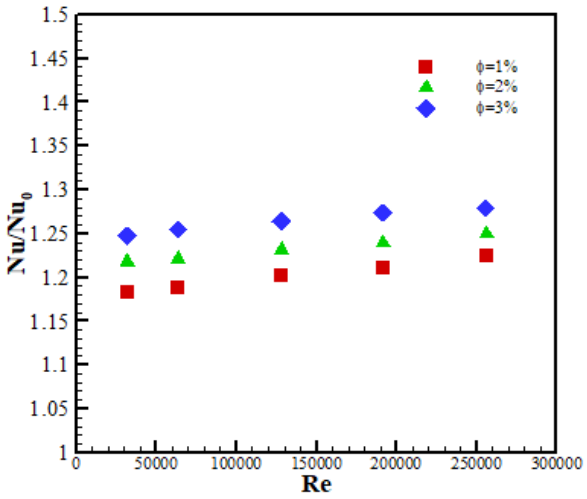

Figure 14. Variation of relative Nusselt number for Al_2O_3–water nanofluid at different volume fractions.

number against Reynolds number for Al_2O_3 nanoparticles at different volume fractions within the base fluid (water). The results clearly indicate that the relative Nusselt number exceeds unity when Al_2O_3 nanoparticles are introduced to the base fluid. This enhancement can be attributed to the significantly improved thermal conductivity of water due to the presence of these nanoparticles. The inclusion of Al_2O_3 nanoparticles transforms the base fluid into a nanofluid, which effectively boosts the heat transfer properties of the fluid.

The study reveals that employing Al_2O_3-water nanofluid as the working fluid within the receiver tube of the collector enhances the thermal performance of the solar system. This improvement is due to the superior heat transfer characteristics offered by nanofluids. As the volume fraction of Al_2O_3 nanoparticles increases, the relative Nusselt number also rises. This behavior is a direct result of the added volume concentration of nanoparticles in the base fluid, which further enhances the fluid's thermal conductivity and augments the Brownian motion of the nanoparticles. These two factors synergistically elevate the thermal performance of the nanofluid, making it significantly more effective in comparison to pure distilled water.

Additionally, the presence of nanoparticles induces micro-convection effects within the fluid due to their constant motion, which contributes to breaking down the thermal boundary layer. This mechanism allows for improved energy transfer between the fluid and the heat-exchanging surfaces. The combined effects of enhanced thermal conductivity, intensified Brownian motion, and micro-convection result in the observed increase in the Nusselt number, demonstrating the superior heat transfer capabilities of Al_2O_3-water nanofluids. These findings underline the importance of optimizing the nanoparticle volume fraction in nanofluids to achieve maximum thermal efficiency in solar systems and other heat exchange applications. By tailoring the nanoparticle concentration and studying its effects on fluid properties, engineers and researchers can develop advanced nanofluids that significantly enhance the performance of thermal systems, paving the way for more efficient and sustainable energy technologies.

Figure 15 illustrates the relationship between the relative friction factor and Reynolds number for Al_2O_3-water nanofluid at various volume fractions of Al_2O_3 nanoparticles. The results highlight the significant impact of adding nanoparticles to pure water on the fluid's viscosity and overall friction factor. In pure water, the viscosity is relatively low, resulting in a lower friction factor. However, the introduction of Al_2O_3 nanoparticles increases the viscosity of the fluid, leading to a relative friction factor greater than one. This indicates that the nanofluid exhibits a higher resistance to flow compared to pure water, which can be attributed to the enhanced interaction between nanoparticles and the base fluid. As shown in figure 15, the relative friction factor increases steadily with higher volume fractions of nanoparticles in the fluid. This trend reflects the combined effects of increased density and viscosity of the nanofluid. The comparatively higher density of the nanofluid, resulting from the presence of dispersed nanoparticles, contributes significantly to the rise in friction factor. Additionally, the enhanced viscosity due to nanoparticle interactions plays a crucial role in increasing flow resistance within the tube. The higher volume fraction of nanoparticles also leads to intensified particle-fluid interactions, which in turn causes more dissipation of energy within the flow. This dissipation further contributes to the increased friction factor observed in nanofluids with greater nanoparticle concentrations. Overall, these findings emphasize the importance of understanding the trade-offs associated with using nanofluids in engineering applications. While the addition of nanoparticles improves the thermal conductivity and heat transfer characteristics of the fluid, the accompanying increase in viscosity and friction factor must be considered to ensure efficient system performance. By carefully optimizing the volume fraction of nanoparticles, engineers and researchers can balance the benefits of enhanced thermal performance with the challenges of increased flow resistance, achieving more effective and sustainable designs for heat exchange and energy systems.

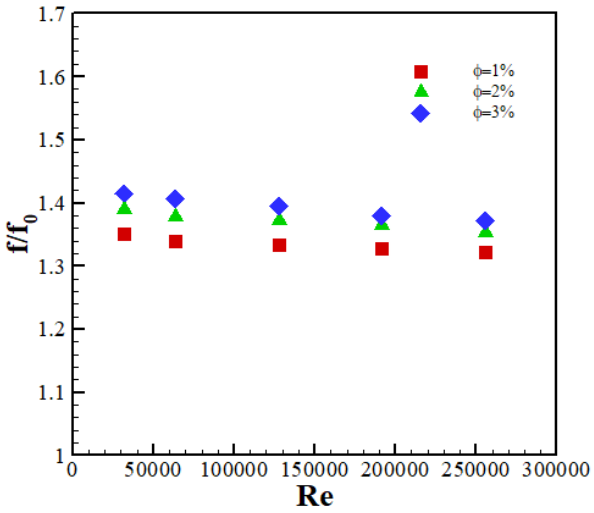

Figure 15. Variation of relative friction factor for Al_2O_3 nanofluid across different volume fractions.

4. Conclusion

In this study, the performance of heat transfer and turbulent fluid flow within tubular receivers using nanofluid was comprehensively analyzed, providing important insights into the influence of various design parameters. The key findings of this research are summarized below:

- The results demonstrated that both the overall Nusselt number and the friction coefficient of the tube increased with an increment in the fin height. This indicates that taller fins enhance heat transfer efficiency while also increasing flow resistance, emphasizing the need to balance these competing effects for optimal system design.
- The computational analysis revealed that the three-dimensional simulations for tubes with a porous fin height of 12 mm required substantially more time 2 and 4 times greater compared to tubes with porous fin heights of 8 mm and 4 mm, respectively. This increase in computational time is attributed to the generation of opposite pressure along the flow direction and the occurrence of flow separation phenomena, which introduce additional complexity to the simulations.
- Results shows that the relative friction factor for Al_2O_3-water nanofluid increases with both Reynolds number and higher nanoparticle volume fractions. This behavior is due to the enhanced viscosity and density of the nanofluid, which improve fluid interaction and energy dissipation, though they also introduce greater flow resistance that must be optimized for efficient system performance.
- It is observed demonstrates that adding Al_2O_3 nanoparticles to water significantly increases the relative friction factor due to enhanced viscosity and density, compared to pure water. As the volume fraction of nanoparticles rises, the friction factor steadily grows, reflecting intensified particle-fluid interactions and energy dissipation, which highlight the trade-offs between improved thermal performance and increased flow resistance in engineering applications.

Authors contributions
Authors have contributed equally in preparing and writing the manuscript.

Availability of data and materials
The authors declare that the data supporting the findings of this study are available within the paper.

Conflict of interests
The authors assert that they do not have any identifiable conflicting financial interests or personal relationships that might be perceived to influence the work presented in this paper.

References

[1] S. A. Kalogirou. "Solar energy engineering: processes and systems.". *Academic press*, 2013.

[2] K. Almutairi, M. A. Nazari, M. Salem, M. M. Rashidi, M. E. H. Assad, and S. Padmanaban. "A review on applications of solar energy for preheating in power plants.". *Alexandria Engineering Journal*, 61(7):5283–94, 2022.
DOI: https://doi.org/10.1016/j.aej.2021.10.045.

[3] O. P. Verma, G. Manik, and S. K. Sethi. "A comprehensive review of renewable energy source on energy optimization of black liquor in MSE using steady and dynamic state modeling, simulation and control.". *Renewable and sustainable energy reviews*, 100:90–109, 2019.
DOI: https://doi.org/10.1016/j.rser.2018.10.002.

[4] İ. H. Yılmaz and M. S. Söylemez. "Design and computer simulation on multi-effect evaporation seawater desalination system using hybrid renewable energy sources in Turkey.". *Desalination*, 291:23–40, 2012.
DOI: https://doi.org/10.1016/j.desal.2012.01.022.

[5] A. K. Hussein. "Applications of nanotechnology in renewable energies—A comprehensive overview and understanding.". *Renewable and Sustainable Energy Reviews*, 42:460–76, 2015.
DOI: https://doi.org/10.1016/j.rser.2014.10.027.

[6] A. K. Hussein. "Applications of nanotechnology to improve the performance of solar collectors.". *Renewable and Sustainable Energy Reviews*, 62:767–92, 2016.
DOI: https://doi.org/10.1016/j.rser.2016.04.050.

[7] O. Younis, A. K. Hussein, M. E. H. Attia, F. L. Rashid, L. Kolsi, and U. Biswal. "Hemispherical solar still: Recent advances and development.". *Energy Reports*, 8:8236–58, 2022.
DOI: https://doi.org/10.1016/j.egyr.2022.06.037.

[8] B. El Ghazzani, D. M. Plaza, R. A. El Cadi, A. Ihlal, B. Abnay, and K. Bouabid. "Thermal plant based on parabolic trough collectors for industrial process heat generation in Morocco.". *Renewable energy*, 113:1261–75, 2017.
DOI: https://doi.org/10.1016/j.renene.2017.06.063.

[9] A. M. Daabo, A. Ahmad, S. Mahmoud, and R. K. Al-Dadah. "Parametric analysis of small scale cavity receiver with optimum shape for solar powered closed Brayton cycle applications.". *Applied Thermal Engineering*, 122:626–41, 2017.
DOI: https://doi.org/10.1016/j.applthermaleng.2017.03.093.

[10] R. Loni, E. A. Asli-Ardeh, B. Ghobadian, and A. Kasaeian. "Experimental study of carbon nano tube/oil nanofluid in dish concentrator using a cylindrical cavity receiver: Outdoor tests.". *Energy Conversion and Management*, 165:593–601, 2018.
DOI: https://doi.org/10.1016/j.enconman.2018.03.079.

[11] F. Razmmand, R. Mehdipour, and S. M. Mousavi. "A numerical investigation on the effect of nanofluids on heat transfer of the solar parabolic trough collectors.". *Applied Thermal Engineering*, 152: 624–33, 2019.
DOI: https://doi.org/10.1016/j.applthermaleng.2019.02.118.

[12] A. Bonanos, M. Georgiou, K. Stokos, and C. Papanicolas. "Engineering aspects and thermal performance of molten salt transfer lines in solar power applications.". *Applied Thermal Engineering*, 154: 294–301, 2019.
DOI: https://doi.org/10.1016/j.applthermaleng.2019.03.091.

[13] M. A. S. Sadjadi, M. Meskinfam, B. Sadeghi, H. Jazdarreh, and K. Zare. "In situ biomimetic synthesis and characterization of nano hydroxyapatite in gelatin matrix.". *Journal of biomedical nanotechnology*, 7(3):450–454, 2011.
DOI: https://doi.org/10.1166/jbn.2011.1305.

[14] M. A. S. Sadjadi, B. Sadeghi, and K. Zare. "Natural bond orbital (NBO) population analysis of cyclic thionylphosphazenes,[NSOX (NPCl2)2]; X= F (1), X= Cl (2).". *Journal of Molecular Structure: THEOCHEM*, 817(1-3):27–33, 2007.
DOI: https://doi.org/10.1016/j.theochem.2007.04.015.

[15] M. Ouagued, A. Khellaf, and L. Loukarfi. "Estimation of the temperature, heat gain and heat loss by solar parabolic trough collector under Algerian climate using different thermal oils.". *Energ. Conver. Manage*, 75:191–201, 2013.
DOI: https://doi.org/10.1016/j.enconman.2013.06.011.

[16] R. V. Padilla, D. Gokmen, Y. Goswami, E. Stefanakos, and M. M. Rahman. "Heat transfer analysis of parabolic trough solar receiver.". *Appl. Energy*, 88(12):5097–5110, 2011.
DOI: https://doi.org/10.1016/j.apenergy.2011.07.012.

[17] R. Forristall. "Heat transfer analysis and modeling of a parabolic trough solar receiver implemented in engineering equation solver.". *National Renewable Energy Lab., Golden, CO.(US)*, NREL/TP-550-34169, 2003.

[18] S. A. Kalogirou. "A detailed thermal model of a parabolic trough collector receiver.". *Energy*, 48(1):298–306, 2012.
DOI: https://doi.org/10.1016/j.energy.2012.06.023.

[19] S. D. Odeh, G. L. Morrison, and M. Behnia. "Modelling of parabolic trough direct steam generation solar collectors.". *Sol. Energy*, 62: 395–406, 1998.

[20] T. Kassem. "Numerical study of the natural convection process in the paraboliccylindrical solar collector.". *Desalination*, 209(1-3): 144–150, 2007.
DOI: https://doi.org/10.1016/j.desal.2007.04.023.

[21] G. Gong, X. Huang, J. Wang, and M. Hao. "An optimized model and test of the China's first high temperature parabolic trough solar receiver.". *Sol. Energy*, 84(12):2230–2245, 2020.
DOI: https://doi.org/10.1016/j.solener.2010.08.003.

[22] J. Lu, J. Ding, J. Yang, and X. Yang. "Nonuniform heat transfer model and performance of parabolic trough solar receiver.". *Energy*, 59:666–675, 2013.
DOI: https://doi.org/10.1016/j.energy.2013.07.052.

[23] Y. L. He, J. Xiao, Z. D. Cheng, and Y. B. Tao. "A MCRT and FVM coupled simulation method for energy conversion process in parabolic trough solar collector.". *Renew. Energy*, 36(3):976–985, 2011.
DOI: https://doi.org/10.1016/j.renene.2010.07.017.

[24] Z. D. Cheng, Y. L. He, F. Q. Cui, R. J. Xu, and Y. B. Tao. "Numerical simulation of a parabolic trough solar collector with nonuniform solar flux conditions by coupling FVM and MCRT method.". *Sol. Energy*, 86(6):1770–1784, 2012.
DOI: https://doi.org/10.1016/j.solener.2012.02.039.

[25] B. Sadeghy and S. Ghammami. "Oxidation of alcohols with tetramethylammonium fluorochromate in aceticoi acid.". *Russian journal of general chemistry*, 75(12):1886–1888, 2005.
DOI: https://doi.org/10.1007/s11176-006-0008-0.

[26] B. Sadeghi, S. Ghammamy, Z. Gholipour, M. Ghorchibeigy, and A. A. Nia. "Gold/hydroxypropyl cellulose hybrid nanocomposite constructed with more complete coverage of gold nano-shell.". *Micro & Nano Letters*, 6(4):209–213, 2011.
DOI: https://doi.org/10.1049/mnl.2011.0036.

[27] A. Amininia, K. Pourshamsian, and B. Sadeghi. "Nano-ZnO Impregnated on Starch—A Highly Efficient Heterogeneous Bio-Based Catalyst for One-Pot Synthesis of Pyranopyrimidinone and Xanthene Derivatives as Potential Antibacterial Agents.". *Russian Journal of Organic Chemistry*, 56(7):1279–1288, 2020.
DOI: https://doi.org/10.1134/S1070428020070234.

[28] Z. D. Cheng, Y. L. He, and Y. U. Qiu. "A detailed nonuniform thermal model of a parabolic trough solar receiver with two halves and two inactive ends.". *Renew. Energy*, 74:139–147, 2015.
DOI: https://doi.org/10.1016/j.renene.2014.07.060.

[29] W. Huang, H. U. Peng, and Z. Chen. "Performance simulation of a parabolic trough solar collector.". *Sol. Energy*, 86(2):746–755, 2012.
DOI: https://doi.org/10.1016/j.solener.2011.11.018.

[30] O. Behar, A. Khellaf, K. Mohammedi, and S. Ait-Kaci. "Effect of Tracking Mode on the Performance of Parabolic Trough Solar Collector.". *University of Bechar*, 2013.

[31] A. C. Ratzel, C. E. Hickox, and D. K. Gartling. "Techniques for reducing thermal conduction and natural convection heat losses in annular receiver geometries.". *J. Heat Transfer*, 101(1):108–113, 1979.
DOI: https://doi.org/10.1115/1.3450899.

[32] K. Reddy and G. Satyanarayana. "Numerical study of porous finned receiver for solar parabolic trough concentrator.". *Engineering applications of computational fluid mechanics*, 2:172–84, 2008.
DOI: https://doi.org/10.1080/19942060.2008.11015219.

[33] M. Bayareh and A. Usefian. "Simulation of parabolic trough solar collectors using various discretization approaches: A review.". *Engineering Analysis with Boundary Elements*, 153:126–37, 2023.
DOI: https://doi.org/10.1016/j.enganabound.2023.05.025.

[34] Y. Shuai, F. Q. Wang, X. L. Xia, and H. P. Tan. "Ray-thermal-structural coupled analysis of parabolic trough solar collector system.". *ISBN*, 2010.

[35] A. K. Tripathy, S. Ray, S. S. Sahoo, and S. Chakrabarty. "Structural analysis of absorber tube used in parabolic trough solar collector and effect of materials on its bending: A computational study.". *Solar Energy*, 163:471–85, 2018.
DOI: https://doi.org/10.1016/j.solener.2018.02.028.

[36] T. Kassem. "Numerical study of the natural convection process in the parabolic-cylindrical solar collector.". *Desalination*, 209(1-3): 144–50, 2007.
DOI: https://doi.org/10.1016/j.desal.2007.04.023.

[37] K. R. Kumar and K. Reddy. "Thermal analysis of solar parabolic trough with porous disc receiver.". *Applied energy*, 86(9):1804–12, 2009.
DOI: https://doi.org/10.1016/j.apenergy.2008.11.007.

[38] S. Gunes, V. Ozceyhan, and O. Buyukalaca. "Heat transfer enhancement in a tube with equilateral triangle cross sectioned coiled wire inserts.". *Experimental Thermal and Fluid Science*, 34(6):684–91, 2010.
DOI: https://doi.org/10.1016/j.expthermflusci.2009.12.010.

[39] E. Bellos, C. Tzivanidis, and D. Tsimpoukis. "Enhancing the performance of parabolic trough collectors using nanofluids and turbulators.". *Renewable and Sustainable Energy Reviews*, 91:358–75, 2018.
DOI: https://doi.org/10.1016/j.rser.2018.03.091.

[40] E. Bellos and C. Tzivanidis. "Enhancing the performance of a parabolic trough collector with combined thermal and optical techniques.". *Applied thermal engineering*, 164:114496, 2020.
DOI: https://doi.org/10.1016/j.applthermaleng.2019.114496.

[41] A. M. Norouzi, M. Siavashi, and M. K. Oskouei. "Efficiency enhancement of the parabolic trough solar collector using the rotating absorber tube and nanoparticles.". *Renewable energy*, 145:569–84, 2020.
DOI: https://doi.org/10.1016/j.renene.2019.06.027.

[42] S. Rashidi, J. A. Esfahani, and A. Rashidi. "A review on the applications of porous materials in solar energy systems.". *Renewable and Sustainable Energy Reviews*, 73:1198–210, 2017.
DOI: https://doi.org/10.1016/j.rser.2017.02.028.

[43] B. Wang, Y. Hong, X. Hou, Z. Xu, P. Wang, and X. Fang. "Numerical configuration design and investigation of heat transfer enhancement in pipes filled with gradient porous materials.". *Energy Conversion and Management*, 105:206–15, 2015.
DOI: https://doi.org/10.1016/j.enconman.2015.07.064.

[44] M. Siavashi, H. R. T. Bahrami, and E. Aminian. "Optimization of heat transfer enhancement and pumping power of a heat exchanger tube using nanofluid with gradient and multi-layered porous foams.". *Applied Thermal Engineering*, 138:465–74, 2018.
DOI: https://doi.org/10.1016/j.applthermaleng.2018.04.066.

[45] S. Asiaei, A. Zadehkafi, and M. Siavashi. "Multi-layered porous foam effects on heat transfer and entropy generation of nanofluid mixed convection inside a two-sided lid-driven enclosure with internal heating.". *Transport in Porous Media*, 126:223–47, 2019.
DOI: https://doi.org/10.1007/s11242-018-1166-3.

[46] A. K. Viswanathan and D. K. Tafti. "Detached eddy simulation of turbulent flow and heat transfer in a two-pass internal cooling duct.". *International Journal of Heat and Fluid Flow*, 27(1):1–20, 2006.
DOI: https://doi.org/10.1016/j.ijheatfluidflow.2005.07.002.

[47] S. Ray, A. K. Tripathy, S. S. Sahoo, and S. Singh. "Effect of Inlet Temperature of Heat Transfer Fluid and Wind Velocity on the Performance of Parabolic Trough Solar Collector Receiver: A Computational.". *International Journal of Heat and Technology*, 37(1): 48–58, 2019.
DOI: https://doi.org/10.18280/ijht.370106.

[48] A. Sarangi, A. Sarangi, S. S. Sahoo, R. K. Mallik, S. Ray, and S. M. Varghese. "A review of different working fluids used in the receiver tube of parabolic trough solar collector.". *Journal of Thermal Analysis and Calorimetry*, 148:3929–3954, 2023.
DOI: https://doi.org/10.1007/s10973-023-11991-y.

[49] Y. Wang, Q. L, J. Lei, and H. Jin. "Performance analysis of a parabolic trough solar collector with non-uniform solar flux conditions.". *International Journal of Heat and Mass Transfer*, 82: 236–249, 2015.
DOI: https://doi.org/10.1016/j.ijheatmasstransfer.2014.11.055.

[50] Y. Qiu, M-J. Li, Y-L. He, and W-Q. Tao. "Thermal performance analysis of a parabolic trough solar collector using supercritical CO2 as heat transfer fluid under non-uniform solar flux.". *Applied Thermal Engineering*, 115:1255–1265, 2017.
DOI: https://doi.org/10.1016/j.applthermaleng.2016.09.044.

[51] M. Klein. "An attempt to assess the quality of large eddy simulations in the context of implicit filtering.". *Flow, Turbulence and Combustion*, 75(1-4):131–147, 2005.
DOI: https://doi.org/10.1007/s10494-005-8581-6.

[52] S. B. Pope. "Turbulent flows.". *New York, NY: Cambridge University Press*, 2000.
DOI: https://doi.org/10.1017/CBO9780511840531.

[53] M. Klein. "An attempt to assess the quality of large eddy simulations in the context of implicit filtering.". *Flow Turbul Combust*, 75(1-4): 131–147, 2005.
DOI: https://doi.org/10.1007/s10494-005-8581-6.

[54] I. B. Celik, Z. N. Cehreli, and I. Yavuz. "Index of resolution quality for large eddy simulations.". *J Fluid Eng*, 127(5):949–958, 2005.
DOI: https://doi.org/10.1115/1.1990201.